Elucidation of Carbohydrate Molecular Interaction Mechanism of Recombinant and Native ArtinM

ARTICLE *in* THE JOURNAL OF PHYSICAL CHEMISTRY B · JUNE 2013

Impact Factor: 3.3 · DOI: 10.1021/jp403087p · Source: PubMed

6 AUTHORS, INCLUDING:

Paulo Roberto Bueno
São Paulo State University
176 PUBLICATIONS **3,397** CITATIONS
SEE PROFILE

Naira Canevarolo Pesquero
São Paulo State University
6 PUBLICATIONS **39** CITATIONS
SEE PROFILE

Rosa Puchades
Universitat Politècnica de València
186 PUBLICATIONS **3,121** CITATIONS
SEE PROFILE

Angel Maquieira
Universitat Politècnica de València
209 PUBLICATIONS **3,598** CITATIONS
SEE PROFILE

THE JOURNAL OF PHYSICAL CHEMISTRY B

Article

pubs.acs.org/JPCB

Elucidation of Carbohydrate Molecular Interaction Mechanism of Recombinant and Native ArtinM

David Giménez-Romero,*[,†] Paulo R. Bueno,*[,‡] Naira C. Pesquero,[‡] Isidro S. Monzó,[§] Rosa Puchades,[†] and Ángel Maquieira[†]

[†]Institute of Molecular Recognition and Technological Development, Department of Chemistry, Universitat Politècnica de València, Camino de Vera s/n, 46022 Valencia, Spain

[‡]Institute of Chemistry, Department of Physical Chemistry, Universidade Estadual Paulista (UNESP), Rua Prof. Francisco Degni 55, 14800-900 Araraquara, São Paulo, Brazil

[§]Department of Physical Chemistry, University of Valencia, C/Dr Moliner 50, 46100 Burjassot, Valencia, Spain

Supporting Information

ABSTRACT: The quartz crystal microbalance (QCM) technique has been applied for monitoring the biorecognition of ArtinM lectins at low horseradish peroxidase glycoprotein (HRP) concentrations, using a simple kinetic model based on Langmuir isotherm in previous work.[18] The latter approach was consistent with the data at dilute conditions but it fails to explain the small differences existing in the jArtinM and rArtinM due to ligand binding concentration limit. Here we extend this analysis to differentiate sugar-binding event of recombinant (rArtinM) and native (jArtinM) ArtinM lectins beyond dilute conditions. Equivalently, functionalized quartz crystal microbalance with dissipation monitoring (QCM-D) was used as real-time label-free technique but structural-dependent kinetic features of the interaction were detailed by using combined analysis of mass and dissipation factor variation. The stated kinetic model not only was able to predict the diluted conditions but also allowed to differentiate ArtinM avidities. For instance, it was found that rArtinM avidity is higher than jArtinM avidity whereas their conformational flexibility is lower. Additionally, it was possible to monitor the hydration shell of the binding complex with ArtinM lectins under dynamic conditions. Such information is key in understanding and differentiating protein binding avidity, biological functionality, and kinetics.

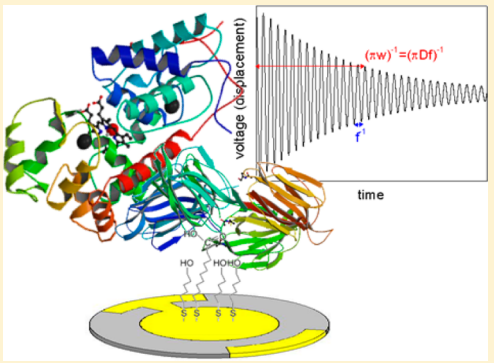

INTRODUCTION

ArtinM, also known as KM+ or Artocarpin, a plant lectin from *Artocarpus integrifolia*[1] belonging to the jacalin-related lectin family, is a tetrameric nonglycosylated protein composed of identical 16 kDa protomers. The protein carbohydrate recognition domains (1 per protomer and 4 per whole protein) preferentially bind to D-mannose, recognizing N-linked glycans containing the trimannoside core Manα1-3[Manα1-6]Man.[2]

Lectin−carbohydrate interactions mediate biological processes such as cell−cell recognition, host−pathogen interactions, cancer metastasis, and cell differentiation. Studies of avidity for carbohydrate together with investigation of carbohydrate structure of glycoproteins by the use of lectins are the main subject for the emerging field of lectinomics and lectin microarrays.[3] Elucidation of carbohydrate selectivity of human and animal lectins is of great importance for better understanding of many biological processes involving cell communication.

ArtinM possesses relevant biological properties. It acts on neutrophils, inducing haptotactic migration and phenotypic and functional changes.[4] Furthermore, an amplification loop for in vivo ArtinM inflammatory activity is provided by induction of mast cell degranulation.[5] ArtinM stimulates macrophage and dendritic cells to release Interleukin 12, thereby establishing in vivo Type 1 helper T cells immunity and conferring protection against several intracellular pathogens.[6] However, evaluation of uses of ArtinM has been limited by the lectin paucity in the extract of *Artocarpus heterophyllus* seeds less than 0.5% of the total protein content.[7] Thus, the abundance of recombinant forms should ease the pharmaceutical application of the ArtinM lectin, as well as the study of its biological properties. The study of native and recombinant lectins compatibility is very important in the medical field, because plant lectins have a limited availability, which would be compensated by the use of recombinant lectins.

Recombinant ArtinM (rArtinM) reproduces well the biological properties of native ArtinM (jArtinM). As jArtinM is a tetramer and rArtinM a monomer, biological functions of both lectins are not identical. For example, jArtinM induces macrophages to produce high levels of pro-inflammatory

Received: March 28, 2013
Revised: June 19, 2013

   dx.doi.org/10.1021/jp403087p | J. Phys. Chem. B XXXX, XXX, XXX−XXX

mediators, but this inflammatory response is not observed with rArtinM stimuli.[8] These discrepancies reinforce the importance of understanding the differences between jArtinM and rArtinM binding features that lead their biological properties and consequently, their pharmacological applications.

The quartz crystal microbalance (QCM-D) is a label-free technique applied to study biological interactions in real-time.[9] It is a versatile mass technique, based on changes in the resonance frequency of the piezoelectric quartz crystal that has found applications in a wide variety of fields, including immunology, medicine, and cell biology.[10−13] Further advances have made possible the measurement of not only the adsorbed mass but also the viscoelastic properties of the adhered layer using the dissipation factor D. This QCM-D performance has been used for studying biological systems,[14] proteins,[15] cellular,[16] and molecular interactions.[17]

The QCM technology has been applied for monitoring the biorecognition of ArtinM at low horseradish peroxidase glycoprotein (HRP) concentrations,[18] using a simple kinetic model based on Langmuir isotherms. This model was consistent with the data at dilute conditions, but it fails to explain the small differences existing in the jArtinM and rArtinM. Therefore, the main goal of the present paper is to evaluate the native and recombinant ArtinM binding properties beyond the dilute limit, in order to better understand the differences in their biological functions. For that, the mass and viscoelastic properties of adsorbed molecules (lectin: ArtinM binding horse radish peroxidase) on a quartz/gold surface while flowing reagent are monitored by QCM-D. Thus, it is provided an independent measure of protein binding kinetics and associated molecular masses.

EXPERIMENTAL METHODS

Instrumental. The QCM-D measurements were carried out in a QCM-D (Q-SENSE, Gothenburg, SWEDEN) instrument working with AT-cut quartz crystals mounted in an E4 system, using an ISMATEC IPC peristaltic pump at a controlled constant flow of 200 μL min^{-1}. The polished quartz crystals (diameter 16 mm, 5 MHz) were provided by Q-SENSE company with gold electrodes. Prior to the experiments, the gold surface was cleaned with a H_2SO_4 (conc)/H_2O_2 30% (7:3, v/v) freshly prepared solution, rinsed with water and dried in air.

Materials, Chemicals, and Operations. The jArtinM used in this work was extracted from *Artocarpus integrifolia* seeds and isolated by D-mannose affinity chromatography, as previously described.[7] In the case of rArtinM, it was isolated through the same affinity procedure from cultures of *Escherichia coli* BL21 (DE3) Codon Plus-RP transformed with pEXP-KM+, according to the procedure described by da Silva et al.[19]

HRP type VI (Sigma Chemical Co., St. Louis, MO) was used to evaluate native and recombinant ArtinM binding properties. Gelatin (Sigma Chemical Co.) was employed as blocking reagent of the functionalized QCM chip, as previously described.[18] The ArtinM solutions (native and recombinant) were prepared in 0.10 M phosphate buffered solution, pH 7.4, with 0.15 M NaCl (PBS).

Lectin Immobilization Methodology. The methodology employed for lectin immobilization was based on self-assembly monolayer on the gold surface of a piezoelectric quartz crystal transducer. The quartz crystal was incubated for 3h in an ethanolic solution containing 10^{-4} M 11-mercaptoundecanoic acid (MUA) and 10 M 2-mercaptoethanol (used as spacer), and then washed with ethanol and PBS. Afterward, it was incubated for 2 h in ethyl(dimethylaminopropyl) carbodiimide/*N*-hydroxysuccinimide solution (10^{-2} and 2.0×10^{-2} M, respectively) and washed with PBS. Finally, the quartz crystal was exposed to the lectin solution (150 mg/L of ArtinM) for 2 h and rinsed with PBS. To block residual carboxylic groups, the lectin-modified crystal surface was exposed to a 0.001% (w/v) gelatin solution for 1 min and washed with PBS. The negative control was the same self-assembly surface without incubation with protein. Therefore, after blocking with gelatin solution, there is no specific interaction of the surface with HRP.

RESULTS AND DISCUSSION

The jArtinM and rArtinM binding properties are evaluated here considering the following reaction scheme for the QCM-D data interpretation (see Figure 1A in Appendix A of the Supporting Information):

$$\begin{aligned} L_{weak} + HRP &\xrightarrow{k_1} L(HRP)_{weak} \\ &\xrightarrow{k_2} L(HRP)_{tight} + HRP \\ &\xrightarrow{k_3} L(HRP)_{2,weak} \\ &\xrightarrow{k_4} L(HRP)_{2,tight} \end{aligned} \quad (1)$$

where $L(HRP)_{weak}$ and $L(HRP)_{tight}$ are weakly (intermediate states) and tightly (reaction products) binding conformations of the lectin (L) and k_i are average kinetic constants. This reaction scheme shows a two-step binding mechanism for each protein carbohydrate recognition domain, as proposed by Amin et al.[20] The reaction schemes of active sites for native (tetramer) and recombinant (monomer) ArtinM lectins may be very similar because all the binding sites have similar structures,[21] and the molecular interaction depends directly on it. In fact, the avidity of both lectins for HRP molecules is analogous although one is a tetramer and the other a monomer.[18]

The jArtinM is a tetramer lectin which can be crystallized in different forms. The form I has dimensions of a = 69.88 Å, b = 73.74 Å, and c = 60.64 Å, whereas the form II has dimensions of a = 43.84 Å, b = 72.19 Å, and c = 46.31 Å.[22] jArtinM structure is not unique, but it changes depending on the state in which it is. Accordingly, jArtinM dimensions indicate that, according to the HRP size (a = 40.28 Å, b = 67.46 Å, and c = 117.11 Å),[23] each immobilized molecule can react only with two HRP molecules due to steric hindrance.

The rArtinM is a monomeric lectin, containing only one glycoprotein binding site. At these experimental conditions, the separation between neighboring rArtinM molecules is about 20 Å, because ArtinM lectins are efficiently immobilized (coating percentage about 63%, as commented below). Hence, due to the HRP size, the rArtinM lectins are also supposed to interact with at least two different average association constants, because neighboring rArtinM molecules may have different binding properties due to steric hindrance. The QCM-D data are simulated adequately considering only two different association processes for rArtinM lectin and therefore, it is not necessary to use new simulation terms that would introduce uncertainty in the determination of simulation coefficients, as it is shown in Figures 2A and 3A (Appendix A in the Supporting Information). At these experimental conditions, if only one association process for the rArtinM lectin is considered, the

dx.doi.org/10.1021/jp403087p | J. Phys. Chem. B XXXX, XXX, XXX−XXX

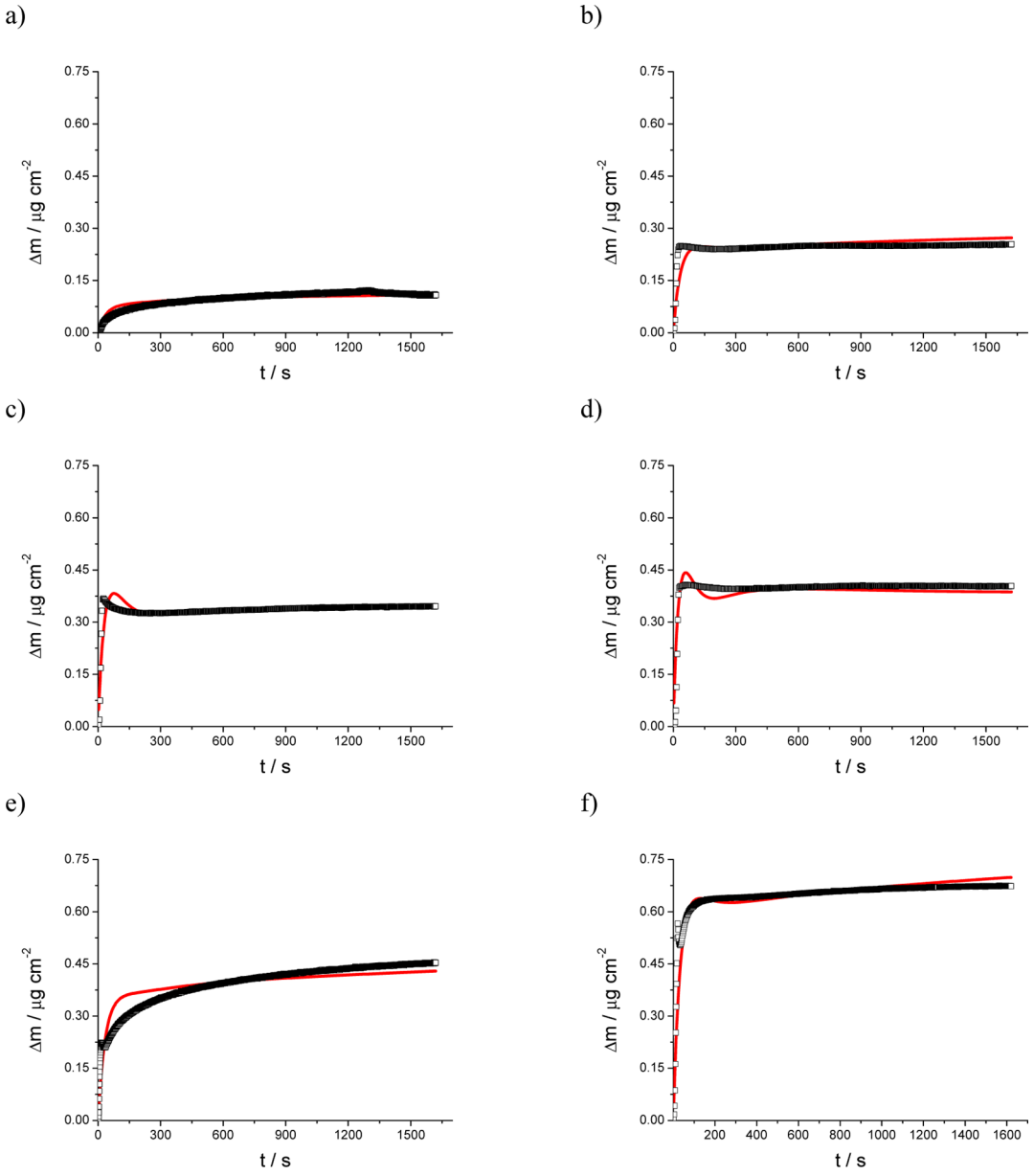

Figure 1. Real-time relaxation curves (Δm shifts as a function of time) of jArtinM−HRP interaction for different HRP concentrations. (a) 0.15 mM, (b) 0.22 mM, (c) 0.40 mM, (d) 0.65 mM, (e) 1.00 mM, and (f) 1.50 mM. The values were obtained in triplicate. The red points are the fittings from the kinetic parameters shown in Table 1.

experimental data cannot be fitted from the reaction scheme proposed by Amin et al.[20]

The physicochemical model and mathematical tools describing this reaction scheme is developed in detail in eqs A.2−A.15 of Appendix A in the Supporting Information, where it is also theoretically shaped to the signals yielded by the QCM-D. Figures 1 and 2 show the plots for jArtinM-HRP and rArtinM-HRP kinetic binding processes, respectively. As can be seen, the trends of plots for both ArtinM forms are very similar. Both real-time kinetic series data show an asymptotic trend respect to the reaction time. Furthermore, the detected HRP amount (adsorbed mass on the bioreactive ArtinM film) increases linearly as the HRP concentration increases. However, for both ArtinM forms this trend is broken when the biorecognition operates at high HRP concentrations (>0.65 mM, undiluted conditions). For example, there is an inflection point on the curves and the adsorbed mass at 1 mM HRP concentration is lower than expected. This fact indicates that HRP starts to agglomerate when concentration of 0.65 mM is reached, decreasing the free HRP in solution that can react with ArtinM lectins. Considering that the molecular recognition depends on its tertiary structure, the following experimental remarks are observed: (i) Changes observed in Figures 1 and 2 are only due to HRP concentration. The ArtinM coverage is approximately constant. (ii) The decrease on adsorbed mass does not depend on the ArtinM form; both have the same trend (an inflection point) for equivalent HRP concentration. (iii) At low HRP concentrations, the QCM-D plot is asymptotic. This behavior is also observed at 1 mM HRP concentration. However, a peak at ≅20 s appears when HRP concentration is between 0.40 and 0.65 mM. The proposed mathematical model, eq A.17 of Appendix A in the Supporting Information, indicates that the absence of local peaks in the QCM-D plot is due to the fact that $k_1 N_{HRP,O} < k_2$. Thus,

dx.doi.org/10.1021/jp403087p | J. Phys. Chem. B XXXX, XXX, XXX−XXX

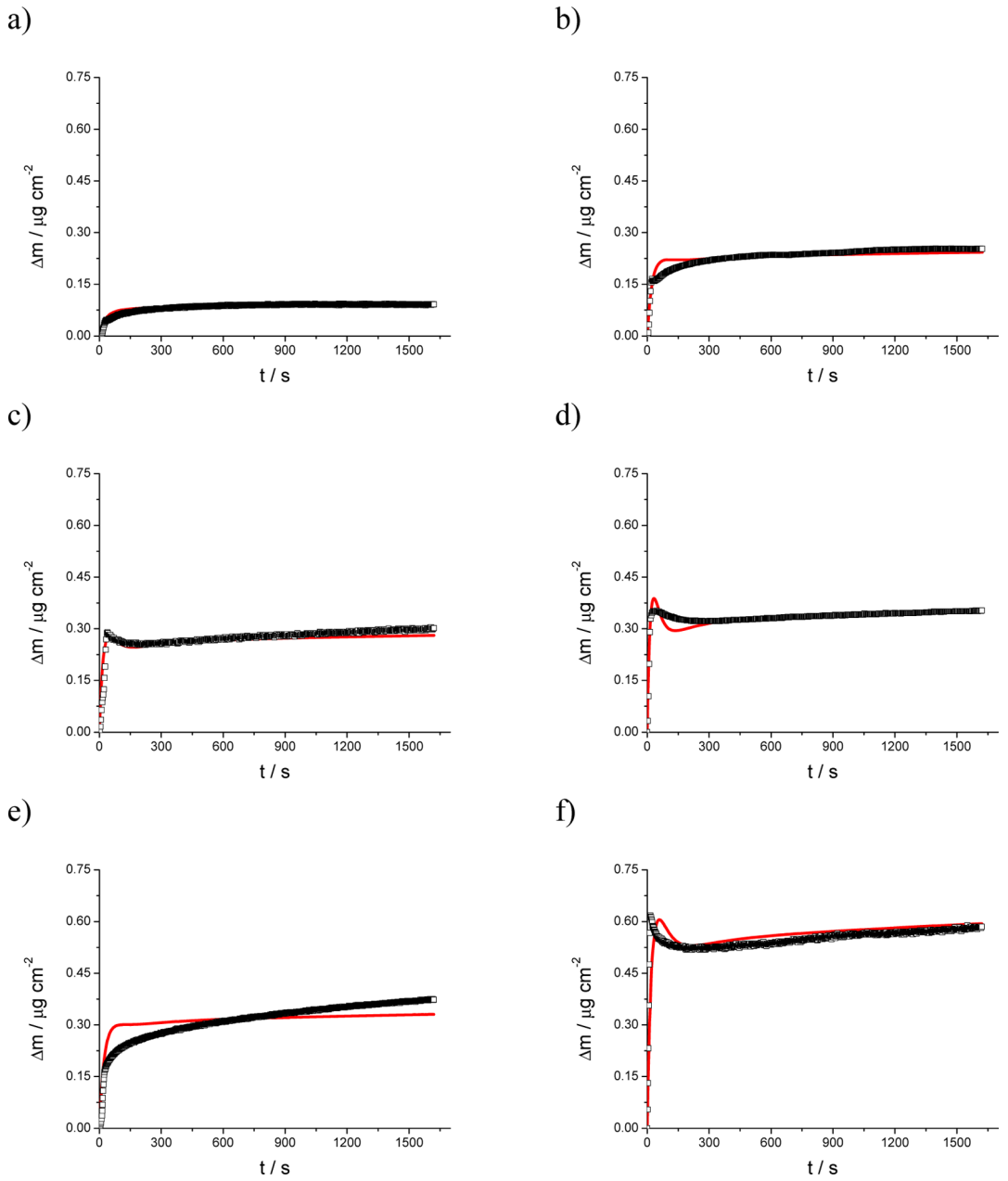

Figure 2. Real-time relaxation curves (Δm shifts as a function of time) of rArtinM−HRP interaction for different HRP concentrations. (a) 0.15 mM, (b) 0.22 mM, (c) 0.40 mM, (d) 0.65 mM, (e) 1.00 mM, and (f) 1.50 mM. The values were obtained in triplicate. The red points are the fittings from the kinetic parameters shown in Table 2.

$k_1N_{HRP,O} < k_2$ operates for HRP concentration up to 1.00 mM, whereas $k_1N_{HRP,O} > k_2$ operates between 0.40 and 0.65 mM, where local peaks are evidenced. Hence, as k_1 and k_2 are constant, $N_{HRP,O}$ (nonaggregated HRP molecules in solution) is lower for HRP concentration 1.00 mM than for HRP 0.40 and 0.65 mM concentration range, where $k_1N_{HRP,O} > k_2$.

Sun et al.[24] described the presence of HRP aggregates in an amorphous structure at higher HRP concentration levels. However, traces of aggregates were observed for most HRP diluted environment, mainly as dimers.[25] Tsaprailis et al.[26] observed that HRP starts precipitating for concentrations higher than 0.1 mM and no aggregation is observed for concentrations lower than 0.03 mM. For similar proteins, a competition between folding and aggregation has also been reported.[27]

All these experiments suggest that HRP aggregation occurs at a critical concentration ranging from 0.65 to 1 mM, influencing the ArtinM-HRP binding. This agglomeration has been reported by other authors.[28] On that basis, the analysis of experimental data evidence the existence of two HRP concentration kinetic regimes, one for no aggregation and other for aggregation. The ArtinM molecules bind strongly to nonaggregated HRP molecules. However, the HRP amorphous aggregates can hardly bind to ArtinM lectins because molecular recognition depends on the protein tertiary structure. In the proposed model, for concentrations higher than the critical, the aggregates are HRP dimers kinetically controlled by first dimerization/agglomeration constant, k_{eq}.

Usually fittings are performed by considering only the system reproducibility. If our experimental data are treated this

dx.doi.org/10.1021/jp403087p | J. Phys. Chem. B XXXX, XXX, XXX−XXX

Table 1. Parameters Calculated from the Fittings of QCM-D Data Obtained for jArtinM-HRP Biorecognition Event in 0.1 M PBS (pH 7.4) Medium

[HRP] mM	k_1 s^{-1} M^{-1}	k_2 s^{-1}	k_3 s^{-1} M^{-1}	k_4 s^{-1}	$MW_{L(HRP)_{weak}}$ kDa	$MW_{L(HRP)_{tight}}$ kDa	$MW_{L(HRP)_{2,weak}}$ kDa	$MW_{L(HRP)_{2,tight}}$ kDa	$N_{L_{weak},0}$ pmol cm^{-2}	K_{eq} M^{-1}
1.50	32.17	0.02772	1.666	0.00978	178.3	32.62	235.1	51.8	15.4	10870.0
1.00	32.27	0.02842	1.688	0.00981	176.6	32.51	237.5	50.9	9.9	10939.9
0.65	31.95	0.02878	1.692	0.00961	158.9	32.87	236.9	52.9	7.2	10971.0
0.40	32.41	0.02857	1.703	0.00997	181.4	32.01	238.0	50.6	7.1	10950.4
0.22	32.50	0.02835	1.670	0.01000	182.0	31.84	236.2	50.3	6.3	10975.5
0.15	32.32	0.02841	1.692	0.00978	176.0	32.48	237.5	50.9	2.6	10964.9
mean	32.3	0.0284	1.69	0.0098	176	32.4	237	51	8	10950
CI[a]	0.2	0.0004	0.01	0.0001	9	0.4	1	1	3	40

[a]Confidence interval.

Table 2. Parameters Calculated from the Fittings of QCM-D Data Obtained for rArtinM-HRP Biorecognition Event in 0.1 M PBS (pH 7.4) Medium

[HRP] mM	k_1 s^{-1} M^{-1}	k_2 s^{-1}	k_3 s^{-1} M^{-1}	k_4 s^{-1}	$MW_{L(HRP)_{weak}}$ kDa	$MW_{L(HRP)_{tight}}$ kDa	$MW_{L(HRP)_{2,weak}}$ kDa	$MW_{L(HRP)_{2,tight}}$ kDa	$N_{L_{weak},0}$ pmol cm^{-2}	K_{eq} M^{-1}
1.50	82.9	0.04087	0.6773	0.005128	173.4	51.5	236.93	79.20	9.5	9000.0
1.00	81.3	0.04100	0.6751	0.005091	155.8	55.7	237.40	79.50	5.2	9000.0
0.65	79.0	0.04100	0.6769	0.005051	156.2	56.1	236.96	79.61	4.7	9000.0
0.40	79.0	0.04114	0.6761	0.005105	149.1	56.5	237.83	79.42	4.0	9000.0
0.22	80.8	0.04117	0.6759	0.005092	154.5	55.6	237.37	79.45	3.8	9000.0
0.15	81.4	0.04104	0.6750	0.005090	156.9	55.9	237.76	79.48	1.4	9001.8
mean	81	0.0410	0.676	0.00509	158	55	237.4	79.4	5	9000.3
CI[a]	2	0.0001	0.001	0.00003	9	2	0.4	0.1	2	0.8

[a]Confidence interval.

manner, fittings are excellent, as shown in Figures 2A and 3A (Appendix A in the Supporting Information, coefficients of determination around 1). However, the confidence interval of the simulation coefficients, when they are calculated at different HRP concentrations, is high, close to 30%. Hence, its physicochemical interpretation is unclear. Herein, the fitting procedure is based on error minimization of the kinetic parameters at different experimental conditions, according to an optimization mathematical routine (written in Wolfram Mathematica 8.0.4. and provided as Appendix B in the Supporting Information).

It should be noted that the fittings in Figures 1 and 2 are performed considering two constraints that are not usually used: (1) the reproducibility of experimental values and (2) the fact that all the simulation coefficients may be constant as the ligand concentration increased. As six simultaneous fittings are made for each ArtinM lectin, the obtained coefficients have a clear physical interpretation. If both constraints were not considered, the physicochemical interpretation of the parameters would be incorrect because it would not consistently predict the evolution of the system. This means that the coefficients would be influenced by the simulation and mathematical randomness, leading to physicochemical misinterpretation. The proposed approach avoids this circumstance and can be applied to the interpretation of kinetic data obtained by other analytical techniques, such as dual polarization interferometry.[29]

Accordingly, Figures 1 and 2 show the good fitting between experimental data and theoretical results, considering this novel strategy. The simulated coefficient values of the ArtinM-HRP interaction as a function of HRP concentrations are given in Tables 1 and 2. The deviations of simulation parameters are low, ranging from 0.2 to 5%, although the average deviation is around 1% (these errors are much lower than those obtained by other mathematical models). Therefore, the simulation coefficients are constant terms as HRP concentration increased. The good fitting of the experimental data, considering the same simulation coefficients for different HRP concentrations, confirms that the binding reaction scheme proposed in eq 1 correctly predict the ArtinM-HRP system behavior over a wide range of HRP concentrations.

The estimated HRP aggregation constants calculated for the jArtinM-HRP (Table 1) and rArtinM-HRP (Table 2) systems are 10940 ± 40 M^{-1} and 9000.3 ± 0.8 M^{-1}, respectively. As expected, the HRP (dimerization) aggregation constant values are equivalent to that found for similar lectins.[30]

The fitting errors are mainly attributed to the lectin immobilization process, B_0, because this is repeated for each individual QCM-D experiment. The results (Tables 1 and 2) indicate that the average coverage apparently does not depend on immobilized ArtinM form, being about 8 ± 3 pmol cm^{-2} for the jArtinM lectin and 5 ± 2 pmol cm^{-2} for rArtinM lectin. Both values are close to the theoretical monolayer coverage, which ranges from approximately 4 to 8 pmol cm^{-2} for jArtinM lectin (taking respectively native forms I and II as reference)[22] and 8 pmol cm^{-2} for rAtinM lectin (taking the recombinant ArtinM structure as reference).[21] This estimated surfacing binding concentration is comparable to that calculated for other similar lectins (this concentration ranges from 14 to 7 pmol cm^{-2}).[31] Hence, it is possible to conclude that ArtinM lectins were efficiently immobilized, as a highly compacted monolayer, in agreement with results obtained previously for analogous lectins.[32]

Furthermore, the first average association constant of ArtinM-HRP biorecognition (Tables 1 and 2) is in the same order of magnitude as that calculated in a previous paper (28 ±

dx.doi.org/10.1021/jp403087p | J. Phys. Chem. B XXXX, XXX, XXX−XXX

4 M^{-1} s^{-1}) for HRP diluted conditions,[18] confirming the results here obtained for a more complete and complex model. The new approach allows considering more aspects of the biorecognition process than the previous one, evidencing small differences that passed unnoticed. Thus, the model demonstrates that jArtinM and rArtinM forms have two different HRP binding sites with two binding steps each at these experimental conditions. Both have different average association constants ($k_1 \neq k_3$). As stated previously, these two recognition active sites agree with the HRP size (a = 40.28 Å, b = 67.46 Å, and c = 117.11 Å)[23] according to steric effects. As both recognition domains are identical,[22] the fact that $k_1 \neq k_3$ implicates that the occupation of the first site affects the second one, meaning that the binding sites have significantly different avidities due to sequential occupation (the interactions are not independent). In other words, although equivalent, the first molecular occupation is favored over the second one due to steric effects, as kinetic values demonstrated ($k_1 > k_3$).

On the other hand, as $k_1 > k_2$, the intermediate state $L(HRP)_{weak}$ can be stabilized depending on the experimental conditions. The model proposed in Appendix A in the Supporting Information, eq A.17, establishes that the peaks observed on QCM-D plots correspond to the presence of a significant amount of this intermediate state. These peaks can be found at short times (about 20s) (Figures 1 and 2). Thus, the intermediate state $L(HRP)_{weak}$ can be easily monitored, characterized, and isolated whether the reaction time is considered. Hence, this state can be strategically modified as convenient, entailing an enormous potential for practical applications.

The first average avidity constant to HRP for rArtinM is higher than k_1 for jArtinM ($k_1^{rArtinM} > K_1^{jArtinM}$, Tables 1 and 2). This result is very interesting, demonstrating that the avidity of rArtinM for glycans is higher than that of jArtinM, allowing the use of the recombinant form instead of the native as a therapeutic tool. However, the biological activity still depends largely on structural changes induced by the ArtinM-glycoprotein recognition, which cannot be determined by means of a simple study on the binding capability.

The modeling of QCM-D experimental analyses (Tables 1 and 2) also provide the molecular weight of the hydrated state of ligand (MW_i). These data indicate that the induced-fit scenario is appropriate to describe the ArtinM-HRP interaction because the population-shift scenario establishes intermediate states without HRP molecules, the closed form without ligand (UC, $MW_{L(HRP)_{weak}}^{population\text{-}shift} = 0$ and $MW_{L(HRP)_{2,weak}}^{population\text{-}shift} = 0$).

The coupling between the protein binding and the conformational transition is explained through two mechanisms: induced-fit and population-shift.[33,34] In the induced-fit scenario, a protein sitting at the open conformer on the unbound surface binds the ligand to jump onto the bound surface, which is followed by the conformational change to the closed conformation, that is, the formation of two states on the detection surface. Conversely, in the population-shift scenario, the protein pre-exists in UC at some small probability and this fraction can bind the ligand directly to reach the closed conformation. The majority of the molecules resides in the unbound surface state before binding. Part of this fraction promptly makes the conformational transition to UC state so that the system achieves the equilibrium on the unbound surface. Thus, for the majority, the protein transits from unbound surface to UC, and to bound surface. Hence, only one state can be detected on the detection surface. The question is, thus, which is the on-pathway intermediate from unbound surface to closed conformation, bound surface (which suggests the induced-fit) or UC (suggesting the population-shift)?

Hence, QCM-D is a powerful tool for the precise distinction between induced-fit and population-shift scenarios. A scenario where the two limiting mechanisms operate at the same time can be modeled by this approach by means of the $MW_{L(HRP)_{i,weak}}$ value. The relative importance of the two scenarios is determined comparing the molecular masses of species that are monitored on the detection surface. Thus and according to the above explanation, a null $MW_{L(HRP)_{i,weak}}$ value indicates that the population-shift predominates as limiting mechanism, and a no zeroed value corresponds to the induced-fit mechanism.

QCM-D data can be also used for detecting the "velcro" effect, that occurs when one ligand molecule binding to two receptor molecules. The average kinetic constants k_3 and k_4, that is, the average kinetic constants of the second binding process, may be zeroed when this effect happens. The "velcro" effect establishes a second binding process that does not change the mass measured by QCM-D, and therefore, it cannot be detected by this technique. Thus, QCM-D data indicate that the "velcro" effect can be overlooked for simulating experimental data at these experimental conditions, because k_3 and $k_4 > 0$ (see Tables 1 and 2).

The molecular weights (MW_i) given in Tables 1 and 2 were established considering that sugar binding does not lead to any substantial change in the ArtinM lectin structure, according to Pratap et al.[22] Therefore, the changes on MW_i of the hydrated state of the target ligand were considered to be only due to a modification in glycoprotein structure, mainly related to variations on its hydration during the binding process. The hydrodynamically coupled water that can be quantified using QCM-D is the hydration layer of proteins, according to Bingen et al.[35] and Zwang et al.[36] Hence, the amount of water molecules in agreement with this layer corresponds logically to the hydration shell of proteins.

It is known that proteins are surrounded by a hydration shell consisting of mono- or bilayers.[37] The water layer is crucial for the protein activity,[38] because when this is lost, their biological activity disappears.[39] Thus, the hydration shell of each HRP molecule can be estimated by subtracting the molecular weight calculated from QCM-D to the nonhydrated weight obtained from literature. It is assumed that the change in hydration caused by each binding event is a constant value for the same type of molecule.[36] This is a methodology similar to that based on optical mass-sensitive techniques (which commonly detect indirectly the absorbed nonhydrated mass). The mechanically coupled mass measured by QCM-D (which detect the absorbed hydrated mass) is corrected by the optical mass.[35,36]

The calculated molecular weight of the jArtinM form in the intermediate state $L(HRP)_{weak}$ is 176 ± 9 kDa (Table 1), corresponding to a HRP molecule with one monolayer of hydration shell (theoretical value is $MW_{L(HRP)_{weak}} \cong 179$ kDa). This value is in good agreement with the induced-fit mechanism, indicating that the ligand binds to the predominant free conformation, $L(HRP)_{weak}$, followed by a conformational change in the macromolecule to give the reaction product, $L(HRP)_{tight}$. $L(HRP)_{tight}$ of the jArtinM has an estimated $MW_{L(HRP)_{tight}}$ value of 32.4 ± 0.4 kDa, indicating a conformational change. This value is equivalent to that of dehydrated HRP molecular weight (theoretical $MW_{HRP} \cong 44$ kDa). Hence,

dx.doi.org/10.1021/jp403087p | J. Phys. Chem. B XXXX, XXX, XXX−XXX

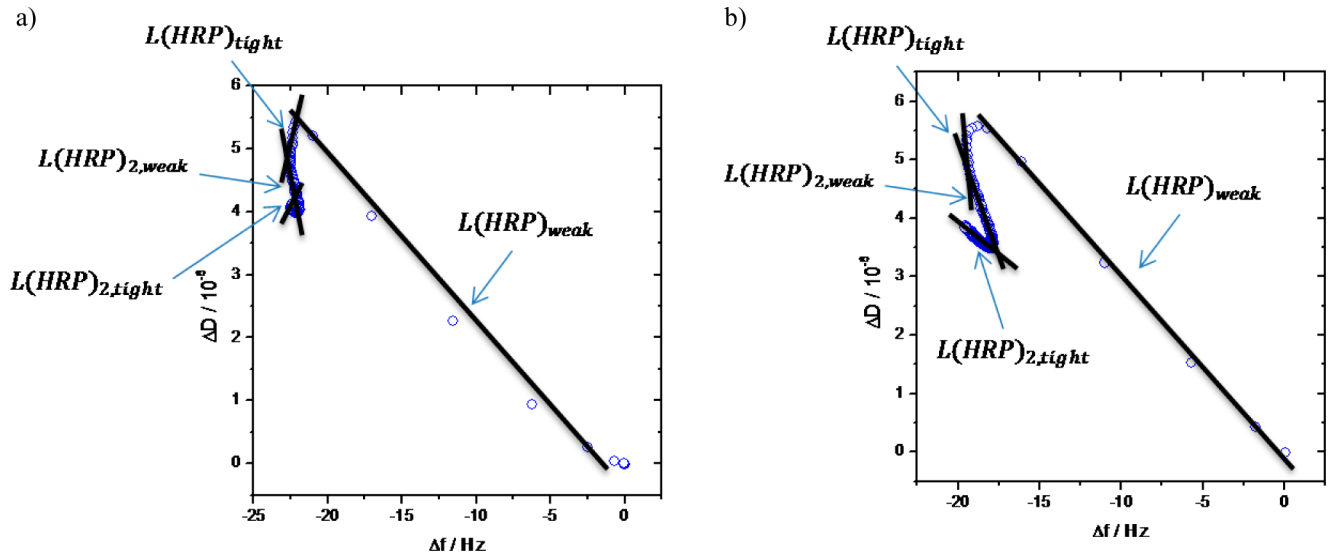

Figure 3. ΔD vs Δf plot obtained during the monitorization of the ArtinM-HRP biorecognition event (0.65 mM HRP in 0.10 M PBS, pH 7.4) for (a) jArtinM and (b) rArtinM.

the conformational change induced by the first HRP−jArtinM interaction decreases the hydration strength of the glycoprotein, eliminating the hydration shell of each HRP molecule and suggesting that ArtinM binds hydrophobically to HRP. Here, it is important to emphasize that the dynamics of the hydration water is sensitive to the distance between proteins[40] and that X-ray data corroborate this dehydration process.[22] The ArtinM dehydration also agrees with the fact that ArtinM−glycoprotein interaction is enthalpically driven and it occurs simultaneously with changes in solvent reorganization shell.[41] Furthermore, this is in agreement with the fact that the binding complex is stabilized mainly by hydrogen bonding and van der Waals interaction, positioning the hydrophilic part of HRP to the protein carbohydrate recognition domain.

The small difference in theoretical ($MW_{L(HRP)_{tight}} \cong 44$ kDa) and experimental ($MW_{L(HRP)_{tight}} \cong 32.4 \pm 0.4$ kDa) values of native $L(HRP)_{tight}$ complex can be attributed to the increase of the viscoelasticity compared to the single molecule theoretical value (due to changes of the adlayer structural properties). An increase in the interfacial viscoelasticity involves a decrease on the estimated value of the mass deposited on QCM-D,[42] lowering the calculated molecular weight.

The viscoelasticity change is confirmed by the obtained dissipation factor values (D). It is important to stress that the observed errors are relatively small because the ΔD vs Δf plot is highly linear and, therefore, it is possible to consider that the studied adlayers are uniform and rigid according to the Sauerbrey equation.

For the second available protein carbohydrate recognition domain, the process of eliminating the hydration shell occurs equivalently (Table 1). The molecular weight measured by QCM-D of the captured ligand in the intermediate state $L(HRP)_{2,weak}$ for the jArtinM form (237 ± 1 kDa) corresponds to the molecular weight of a HRP molecule with a monolayer of hydration shell plus the molecular weight of HRP bound to the first preferential domain (theoretical $MW_{L(HRP)_{2,weak}} \cong 223$ kDa). This complex also eliminates its hydration shell during the conformational changes induced in the second ArtinM-HRP binding process, obtaining a value of $MW_{L(HRP)_{2,tight}} \cong 51 \pm 1$ kDa. Again, the discrepancy observed between theoretical (theoretical $MW_{L(HRP)2,tight} \cong 88$ kDa) and estimated values can be attributed to viscoelastic effects.

The elimination of hydration shell observed for the jArtinM−HRP complex also occurs during rArtinM−HRP binding event. The molecular weights of the captured ligands during jArtinM-HRP binding process are similar to that obtained when the binding for rArtinM is evaluated (Tables 1 and 2). Again, the small differences between the biorecognition for jArtinM and rArtinM forms can be attributed to differences on the viscoelasticity of binding complexes involved in eq 1. Despite binding sites of jArtinM and rArtinM have very similar structure,[21] there are inherent local structural differences on recognition domain related to protein expression in another organism, which involve slight fluctuations on the local recognition domain structure.

The QCM-D technique is able to measure mass changes in adlayers and additionally measure viscoelastic properties (the viscous and/or elastic characteristics of materials when undergoing deformation) of the adhered layer using the dissipation factor D (as shown and discussed in Appendix A in the Supporting Information), using the simple ratio deduced in eq A.26. This novel ratio shows how the slope of linear regression of ΔD vs Δf plot (Figure 3) is related to the elasticity of the adhered proteins.

Accordingly, four working ranges can be obtained from the four observed linear intervals for both ArtinM forms. These slopes show how the adhered protein layer changes its elasticity (i.e., its conformational flexibility) depending on the major reaction product, allowing the intermediate states involved in molecular recognition mechanism to be monitored. Therefore, these intervals reinforce the kinetic mechanism proposed in eq 1, which establishes four different reaction products: $L(HRP)_{weak}$, $L(HRP)_{tight}$, $L(HRP)_{2,weak}$, and $L(HRP)_{2,tight}$ The analysis of the dissipation factor data shows that the proposed model extended the simplistic one, broadly used for protein−ligand interaction, stated in a previous paper.[18]

The analysis of D factor additionally provides information for a more practical differentiation of jArtiM and rArtiM structures, due to inherent structural fluctuations during protein expression process. The linear regression of slopes (Figure 3)

dx.doi.org/10.1021/jp403087p | J. Phys. Chem. B XXXX, XXX, XXX−XXX

is related to structural differences of the studied overlayers (see Appendix A in the Supporting Information). The slopes are more positive as the conformational flexibility of adhered proteins increases, and more negative as this conformational flexibility decreases. The slopes of the linear intervals detected during the HRP biorecognition carried out by both jArtinM and rArtinM are listed in Table 3.

Table 3. Slopes of the Lineal Intervals from the ΔD vs Δf plot (Figure 3) Obtained during the Monitorization of the ArtinM-HRP Biorecognition Event

reagent species	$\Delta D/\Delta f^{jArtinM}$ ($\times 10^{-6}$ Hz^{-1})	$\Delta D/\Delta f^{jArtinM}$ ($\times 10^{-6}$ Hz^{-1})
$L(HRP)_{weak}$	−0.20722	−0.3068
$L(HRP)_{tight}$	1.5779	−1.6931
$L(HRP)_{2,weak}$	−1.0194	−0.8062
$L(HRP)_{2,tight}$	0.3662	−0.2348

As shown in Table 3, the conformational flexibility of the $L(HRP)_{weak}$ state is very similar for both ArtinM forms, as expected because it is constituted mainly by the same HRP molecular structure (see Table 3), that has a very weak interaction. In summary, the differences existing between jArtin0M and rArtinM forms during the first binding step are mainly attributed to difference on elasticity of the formed $L(HRP)_{tight}$ complex.

The reaction steps of $L(HRP)_{weak}$ to $L(HRP)_{tight}$ jArtinM states implicate a high increase of the conformational flexibility of the lectin-HRP film (positive slopes), confirming the discussions previously stated. This is also observed during the HRP interaction with the second protomer of jArtinM (Table 3). The above observed difference occurring for $L(HRP)_{weak}$ and $L(HRP)_{tight}$ jArtinM states is confirmed by the analysis of dissipation factor obtained in real time during the binding process. It is important to emphasize that these results allow concluding that the film flexibility increases when native ArtinM−HRP complexes are the major reaction product. Interestingly, if hydrodynamically coupled water influenced the mass measured by QCM-D, the film rigidity would increase with the same rate as the biorecognition process occurs.[43,44] Hence, the increase on the flexibility detected at these experimental conditions demonstrates that binding may induce a significant structural change of the film.[43]

In contrast to jArtinM, the interaction step between $L(HRP)_{weak}$ and $L(HRP)_{tight}$ for rArtinM ligand indicates an increase on the rigidity of adhered protein (more negative slopes), that means a decrease on its conformational flexibility. This opposite effect can be evidenced by the difference found on the slopes of ΔD vs Δf plots, which is more positive for jArtinM (positive value, 1.57×10^6 Hz^{-1}) compared to rArtinM (negative value, -1.69×10^6 Hz^{-1}).

Results shown in Table 3 also demonstrate that the second recognition step for rArtinM is similar to the first step $L(HRP)_{2,tight}$ being more elastic than the $L(HRP)_{tight}$ form. It is important to emphasize that the elasticity of $L(HRP)_{2,tight}$ and $L(HRP)_{weak}$ recombinant forms are very similar (-0.2348×10^6 and -0.3068×10^6 Hz^{-1}, respectively). This is an indication that the rArtinM-HRP tight binding is weak, as happened for $L(HRP)_{weak}$, and in agreement to the fact that steric effects are involved. Accordingly, structural changes induced by the ArtinM−glycoprotein recognition are different in both ArtinM forms. Then, the in vivo function of both lectins is expected to be different although recombinant ArtinM has a higher avidity with glycans compared to the native form; for example, jArtinM induces macrophages to produce high levels of pro-inflammatory mediators but this response is not observed with rArtinM stimuli.[8]

Several remarks based on binding malleability can be pointed out now. It is important to reinforce that elasticity features discussed and observed in jArtinM form are corroborated by studies conducted on the jacalin-related lectin family.[45] This lectin family affects the lipid packing of biological membranes in the presence of glycoconjugates (this effect is not observed when the lipid monolayers have not these glycoconjugates), making the film lesser fluidic. This lectin−glycoconjugate binding contributes to a more rigid and compacted monolayer. The increase of conformational flexibility measured here is in agreement to this fact and indicates that native glycoconjugate are able to work as "expansion joints". Because of its elasticity, the lectin−glycan complex acts as an assembly able to absorb the expansion and contraction induced by the structuration of biological membranes. As a result, the monolayer is directional and rigid (compact). This behavior is supposed to be inhibited when the agglomerated complex, $L(HRP)_{tight}$, is not formed. In other words, the lectin−glycan complex makes possible the packing of the lipid layer, as demonstrated previously by Nobre et al.[45] Note that this could be related to important effects in the cell internalization mechanism that still remains to be elucidated. This conformational flexibility also explains the lectin−glycan interactions involved in many biological processes, such as cell differentiation and epithelial tissue regeneration.

In summary, our results demonstrate that jArtinM and rArtinM have equivalent binding structural features (controlled by induced-fit mechanism), but the rArtinM has higher glycans avidity than native form. Also, their biological functions are not identical, because the viscoelastic (or conformational flexibility) properties of both ArtinM−glycoprotein complexes are different.

CONCLUSIONS

QCM-D technique has made to map out the relevant conformational states of ArtinM−glycoprotein binding with the purpose to develop a mechanistic structural-based model, able to deal with kinetic real-time binding curves beyond diluted limit of the ligand (with induced-fit mechanism dominating). Hydration shells of binding proteins and intermediate states were found to play a key role on the understanding of ArtinMs bindings, allowing a more precise comparison between the biological behavior of jArtinM and rArtinM lectins. This comparison has been reached using the D factor, because it allows elementary reactions involved in molecular recognition mechanisms, as well as its intermediate states, to be monitored.

Hydration of each lectin−glycoprotein complex molecule is crucial to differentiate the HRP binding event of jArtinM and rArtinM. The ArtinM recognition domain site binding is strongly blocked or intermediated by glycoprotein hydrophobic part. Therefore, although rArtinM presents higher avidity by glycans, the worse biological functionality of recombinant lectins[46] can be attributed to malleability differences in the recognition sites. The conformational flexibility of jArtinM is higher than that of the rArtinM form, which can explain the higher biological functionality of the native form, as well as the "expansion joints" effect. The proposed model explains why the

dx.doi.org/10.1021/jp403087p | J. Phys. Chem. B XXXX, XXX, XXX−XXX

native ArtinM cannot be completely replaced by its recombinant form.

As a final conclusion, the proposed induced-fit mechanism can be useful to understand the in vivo function of native and recombinant lectins, and other protein binding events could be comprehensively evaluated on the future using this approach. Furthermore, the QCM-D sensor was used, for the first time, to monitor the evolution of the hydration shell of protein during a biorecognition reaction.

■ ASSOCIATED CONTENT

Supporting Information

Physicochemical model and mathematical tools describing the proposed reaction scheme is developed in detail in Appendix A. Appendix B provides the multiobjective optimization routine proposed in this manuscript, which is written in Wolfram Mathematica 8.0.4. This material is available free of charge via the Internet at http://pubs.acs.org

■ AUTHOR INFORMATION

Corresponding Author

*(P.R.B.) Phone: +55 16 3301 9642. Fax: +55 16 3322 2308. E-mail: prbueno@iq.unesp.br. (D.G.-R.) Phone: +34 96 387 73 42. Fax: +34 96 3879 349. E-mail: giroda@qim.upv.es.

Notes

The authors declare no competing financial interest.

■ ACKNOWLEDGMENTS

P.R.B. acknowledges FAPESP (São Paulo State Research Fund Agency) for the financial support and all grant projects related to. This research was also funded through project Feder CTQ2010-15943 (CICYT, Spain), GVA ACOMP-2009/650, GVA Prometeo 2010/008, and PAID-06-12 (Universitat Politècnica de València). D.G.-R. acknowledges his position to the "Ramon y Cajal" Program (Spanish Ministry of Economy and Competitiveness). We are very grateful to Prof. Dra. Maria Cristina Roque Barreira and her group for providing ArtinM lectins used in this work and to David Gimenez-Pastor for his immense patience.

■ REFERENCES

(1) Pereira-da-Silva, G.; Roque-Barreira, M. C.; Van Damme, E. J. Artin M: A rational substitution for the names artocarpin and KM+. *Immunol. Lett.* **2008**, *119*, 114−115.

(2) Jeyaprakash, A. A.; Srivastav, A.; Surolia, A.; Vijayan, M. Structural Basis for the Carbohydrate Specificities of Artocarpin: Variation in the Length of a Loop as a Strategy for Generating Ligand Specificity. *J. Mol. Biol.* **2004**, *338*, 757−770.

(3) Gemeiner, P.; Mislovičová, D.; Tkáč, J.; Švitel, J.; Pätoprstý, V.; Hrabárová, E.; Kogan, G.; Kožár, T. Lectinomics: II. A highway to biomedical/clinical diagnostics. *Biotechnol. Adv.* **2009**, *27*, 1−15.

(4) Ganiko, L.; Martins, A. R.; Freymuller, E.; Mortara, R. A.; Roque-Barreira, M. C. Lectin KM+-induced neutrophil haptotaxis involves binding to laminin. *Biochim. Biophys. Acta, Gen. Subj.* **2005**, *1721*, 152−163.

(5) Moreno, A. N.; Jamur, M. C.; Oliver, C.; Roque-Barreira, M. C. Mast Cell Degranulation Induced by Lectins: Effect on Neutrophil Recruitment. *Int. Arch. Allergy Immunol.* **2003**, *132*, 221−230.

(6) Coltri, K. C.; Oliveira, L. L.; Pinzan, C. F.; Vendruscolo, P. E.; Martinez, R.; et al. Therapeutic Administration of KM+ Lectin Protects Mice Against Paracoccidioides brasiliensis Infection via Interleukin-12 Production in a Toll-Like Receptor 2-Dependent Mechanism. *Am. J. Pathol.* **2008**, *173*, 423−432.

(7) Santos de Oliveira, R.; Dias-Baruffi, M.; Thomaz, S. M. O.; Beltramini, L. M.; Roque- Barreira, M. C. A neutrophil migration-inducing lectin from Artocarpus integrifolia. *J. Immunol.* **1994**, *153*, 1798−1807.

(8) Cecilio, N. T.; Luche, D. D.; Carvalho, F. C.; Fernandes, A. L. V. Z.; Liu, Y.; Feizi, T.; Goldman, M. H. S.; Roque-Barreira, M. C. XXXVII Congress of the Brazilian Society of Immunology, 2012.

(9) Roederer, J. E.; Bastiaans, G. J. Microgravimetric immunoassay with piezoelectric crystals. *Anal. Chem.* **1983**, *55*, 2333−2336.

(10) Marx, K. A. Quartz Crystal Microbalance: A useful tool for studying thin polymer films and complex biomolecular systems at the solution−surface interface. *Biomacromolecules* **2003**, *4*, 1099−1120.

(11) Reuel, N. F.; Mu, B.; Zhang, J.; Hinckley, A.; Stano, M. S. Nanoengineered glycan sensors enabling native glycoprofiling for medicinal applications: towards profiling glycoproteins without labeling or liberation steps. *Chem. Soc. Rev.* **2012**, *41*, 5744−5779.

(12) Chen, C. I.; Chang, Y. P.; Chu, Y. H. Biomolecular interactions and tools for their recognition: focus on the quartz crystal microbalance and its diverse surface chemistries and applications. *Chem. Soc. Rev.* **2012**, *41*, 1947−1971.

(13) Speight, R. E.; Cooper, M. A. A survey of the 2010 Quartz Crystal Microbalance literature. *J. Mol. Recognit.* **2012**, *25*, 451−473.

(14) Rodahl, M.; Hook, F.; Fredriksson, C.; Keller, C. A.; Krozer, A.; Brzezinski, P.; Voinova, M.; Kasemo, B. Simultaneous frequency and dissipation factor QCM measurements of biomolecular adsorption and cell adhesion. *Faraday Discuss.* **1997**, *107*, 229−246.

(15) Roach, P.; Farrar, D.; Perry, C. Interpretation of protein adsorption: Surface-induced conformational changes. *J. Am. Chem. Soc.* **2005**, *127*, 8168−8173.

(16) Li, J.; Thielemann, C.; Reuning, U.; Johannsmann, D. Monitoring of integrin-mediated adhesion of human ovarian cancer cells to model protein surfaces by quartz crystal resonators: evaluation in the impedance analysis mode. *Biosens. Bioelectron.* **2005**, *20*, 1333−1340.

(17) Pei, Z.; Anderson, H.; Aastrup, T.; Ramstrom, O. Study of real-time lectin−carbohydrate interactions on the surface of a quartz crystal microbalance. *Biosens. Bioelectron.* **2005**, *21*, 60−66.

(18) Pesquero, N. C.; Pedroso, M. M.; Watanabe, A. M.; Goldman, M. H. S.; Faria, R. C.; Roque-Barreira, M. C.; Bueno, P. R. Real-time monitoring and kinetic parameter estimation of the affinity interaction of jArtinM and rArtinM with peroxidase glycoprotein by the electrogravimetric technique. *Biosens. Bioelectron.* **2010**, *26*, 36−42.

(19) da Silva, L. L.; Molfetta-Machado, J. B.; Panunto-Castelo, A.; Denecke, J.; Goldman, G. H.; Roque-Barreira, M. C.; Goldman, M. H. cDNA cloning and functional expression of KM+, the mannose-binding lectin from Artocarpus integrifolia seeds. *Biochim. Biophys. Acta, Gen. Subj.* **2005**, *1726*, 251−260.

(20) Amin, S. K. R.; Banerjee, S.; Kasturi, S. R.; Chatterjee, B. P. Binding mechanism of methyl-alpha-n-acetyl-d-galactopyranosyl amine to Artoca. *Indian J. Biochem. Biophys.* **2000**, *37*, 299−306.

(21) Pranchevicius, M. C. S.; Oliveira, L. L.; Rosa, J. C.; Avanci, N. C.; Quiapin, A. C.; Roque-Barreira, M. C.; Goldman, M. H. S. Characterization and optimization of ArtinM lectin expression in Escherichia coli. *BMC Biotechnol.* **2012**, *12*, 44.

(22) Pratap, J. V.; Jeyaprakash, A. A.; Rani, P. G.; Sekar, K.; Surolia, A.; Vijayan, M. Crystal structures of artocarpin, a Moraceae lectin with mannose specificity, and its complex with methyl-α-d-mannose: implications to the generation of carbohydrate specificity. *J. Mol. Biol.* **2002**, *317*, 237−247.

(23) Berglund, G. I.; Carlsson, G. H.; Smith, A. T.; Szoke, H.; Henriksen, A.; Hajdu, J. The catalytic pathway of horseradish peroxidase at high resolution. *Nature* **2002**, 417−463.

(24) Sun, J.; Sun, F.; Xu, B.; Gu, N. The quasi-one-dimensional assembly of horseradish peroxidase molecules in presence of the alternating magnetic field. *Colloids Surf., A* **2010**, *360*, 94−98.

(25) Delincée, H.; Radola, B. J. Effect of γ-Irradiation on the Charge and Size Properties of Horseradish Peroxidase: Individual Isoenzymes. *Radiat. Res.* **1974**, *59*, 572−584.

(26) Tsaprailis, G.; Chan, D.; English, A. M. Conformational States in Denaturants of Cytochrome c and Horseradish Peroxidases Examined by Fluorescence and Circular Dichroism. *Biochemistry* **1998**, *37*, 2004−2016.
(27) Garel, J.-R. In *Protein Folding*, first ed.; Creighton, T. E., Ed.; W.H. Freeman: New York, 1992; pp 405−454.
(28) Morris, A. M.; Watzky, M. A.; Finke, R. G. Protein aggregation kinetics, mechanism, and curve-fitting: A review of the literature. *Biochim. Biophys. Acta, Proteins Proteomics* **2009**, *1794*, 375−397.
(29) Gimenez-Romero, D.; Gonzalez-Martinez, M. A.; Bañuls, M. J.; Monzo, I. S.; Puchades, R.; Maquieira, A. Modeling of the role of conformational dynamics in kinetics of the antigen−antibody interaction in heterogeneous phase. *J. Phys. Chem. B* **2012**, *116*, 5679−5688.
(30) Hoggett, J. G.; Kellett, G. L. Kinetics of the monomer-dimer reaction of yeast hexokinase PI. *Biochem. J.* **1992**, *287*, 567−572.
(31) Hirabayashi, J.; Yamada, M.; Kuno, A.; Hiroaki, T. Lectin microarrays: concept, principle and applications. *Chem. Soc. Rev.* **2013**, *42*, 4443−4458.
(32) Monzo, A.; Bonn, G. K.; Guttman, A. Lectin-immobilization strategies for affinity purification and separation of glycoconjugates. *TrAC, Trends Anal. Chem.* **2007**, *26*, 423−432.
(33) Volkman, B. F.; Lipson, D.; Wemmer, D. E.; Kern, D. Two-State allosteric behavior in a single-domain signaling protein. *Science* **2001**, *291*, 2429−2433.
(34) Okazaki, K.; Takada, S. Dynamic energy landscape view of coupled binding and protein conformational change: Induced-fit versus population-shift mechanisms. *Proc. Natl. Acad. Sci. U.S.A.* **2008**, *105*, 11182−11187.
(35) Bingen, P.; Wang, G.; Steinmetz, N. F.; Rodahl, M.; Richter, R. P. Solvation effects in the Quartz Crystal Microbalance with dissipation monitoring response to biomolecular adsorption. A phenomenological approach. *Anal. Chem.* **2008**, *80*, 8880−8890.
(36) Zwang, T. J.; Patel, R.; Johal, M. S.; Selassie, C. R. Desolvation of BSA−ligand complexes measured using the Quartz Crystal Microbalance and Dual Polarization Interferometer. *Langmuir* **2010**, *28*, 9616−9620.
(37) Fenimore, P. W.; Freuenfelder, H.; McMahon, B. H.; Young, R. D. Bulk-solvent and hydration-shell fluctuations, similar to α- and β-fluctuations in glasses, control protein motions and functions. *Proc. Natl. Acad. Sci. U.S.A.* **2004**, *101*, 14408−14413.
(38) Brovchenko, I.; Oleinikova, A. Which properties of a spanning network of hydration water enable biological functions? *ChemPhysChem* **2008**, *9*, 2695−2702.
(39) Frauenfelder, H.; Chen, G.; Berendzen, J.; Fenimore, P. W.; Jansson, H.; McMahon, B. H.; Stroe, I. R.; Swenson, J.; Young, R. D. Physical Sciences - Physics - Biological Sciences - Biophysics and Computational Biology. *Proc. Natl. Acad. Sci. U.S.A.* **2009**, *106*, 5129−5134.
(40) Ebbinghaus, S.; Kim, S. J.; Heyden, M.; Yu, X.; Heugen, U.; Gruebele, M.; Leitner, D. M.; Havenith, M. *Proc. Natl. Acad. Sci. U.S.A.* **2007**, *104*, 20749−20752.
(41) Rani, P. G.; Baschhawa, K.; Misquith, S.; Surolia, A. Thermodynamic studies of saccharide binding to Artocarpin, a B-Cell mitogen, reveals the extended nature of its interaction with mannotriose[3,6-Di-O-(α-d-mannopyranosyl)-d-mannose]. *J. Biol. Chem.* **1999**, *274*, 29694−29698.
(42) Kanazawa, K. K.; Gordon, J. G. The oscillation frequency of a quartz resonator in contact with liquid. *Anal. Chim. Acta* **1985**, *175*, 99−105.
(43) Höök, F.; Vörös, J.; Rodahl, M.; Kurrat, R.; Böni, P.; Ramsden, J. J.; Textor, M.; Spencer, N. D.; Tengvall, P.; Gold, J.; Kasemo, B. A comparative study of protein adsorption on titanium oxide surfaces using in situ ellipsometry, optical waveguide lightmode spectroscopy, and quartz crystal microbalance/dissipation. *Colloids Surf., B* **2002**, *24*, 155−170.
(44) Reimhult, E.; Larsson, C.; Kasemo, B.; Höök, F. Simultaneous Surface Plasmon Resonance and Quartz Crystal Microbalance with Dissipation Monitoring Measurements of Biomolecular Adsorption Events Involving Structural Transformations and Variations in Coupled Water. *Anal. Chem.* **2004**, *76*, 7211−7220.
(45) Nobre, T. M.; Pavinatto, F. J.; Cominetti, M. R.; Selistre de-Araujo, H. S.; Zaniquelli, M. E. D.; Beltramini, L. M. The specificity of frutalin lectin using biomembrane models. *Biochim. Biophys. Acta, Biomembr.* **2010**, *1798*, 1547−1555.
(46) Yang, N.; Tong, X.; Xiang, Y.; Zhang, Y.; Liang, Y.; Sun, H.; Wang, D. C. Molecular character of the recombinant antitumor lectin from the edible mushroom *Agrocybe aegerita*. *J. Biochem.* **2005**, *138*, 145−150.